J. Neurovirol.
DOI 10.1007/s13365-017-0530-3

Modeling brain lentiviral infections during antiretroviral therapy in AIDS

Weston C. Roda[1] · Michael Y. Li[1] · Michael S. Akinwumi[1] · Eugene L. Asahchop[2] · Benjamin B. Gelman[3] · Kenneth W. Witwer[4] · Christopher Power[2]

Received: 13 January 2017 / Revised: 7 April 2017 / Accepted: 20 April 2017

Abstract Understanding HIV-1 replication and latency in different reservoirs is an ongoing challenge in the care of patients with HIV/AIDS. A mathematical model was created to describe and predict the viral dynamics of HIV-1 and SIV infection within the brain during effective combination antiretroviral therapy (cART). The mathematical model was formulated based on the biology of lentiviral infection of brain macrophages and used to describe the dynamics of transmission and progression of lentiviral infection in brain. Based on previous reports quantifying total viral DNA levels in brain from HIV-1 and SIV infections, estimates of integrated proviral DNA burden were made, which were used to calibrate the mathematical model predicting viral accrual in brain macrophages from primary infection. The annual rate at which susceptible brain macrophages become HIV-1 infected was estimated to be 2.90×10^{-7}–4.87×10^{-6} per year for cART-treated HIV/AIDS patients without comorbid neurological disorders. The transmission rate for SIV infection among untreated macaques was estimated to be 5.30×10^{-6}–1.37×10^{-5} per year. An improvement in cART effectiveness (1.6–48%) would suppress HIV-1 infection in patients without neurological disorders. Among patients with advanced disease, a substantial improvement in cART effectiveness (70%) would eradicate HIV-1 provirus from the brain within 3–32 (interquartile range 3–9) years in patients without neurological disorders, whereas 4–51 (interquartile range 4–16) years of efficacious cART would be required for HIV/AIDS patients with comorbid neurological disorders. HIV-1 and SIV provirus burdens in the brain increase over time. A moderately efficacious antiretroviral therapy regimen could eradicate HIV-1 infection in the brain that was dependent on brain macrophage lifespan and the presence of neurological comorbidity.

Keywords Mathematical model · Viral dynamics · Brain macrophage · HIV-1 · SIV · Combination antiretroviral therapy (cART)

Electronic supplementary material The online version of this article (doi:10.1007/s13365-017-0530-3) contains supplementary material, which is available to authorized users.

✉ Michael Y. Li
mli@math.ualberta.ca

Weston C. Roda
weston.roda@gmail.com

Michael S. Akinwumi
segunmic@ualberta.ca

Eugene L. Asahchop
asahchop@ualberta.ca

Benjamin B. Gelman
bgelman@utmb.edu

Kenneth W. Witwer
kwitwer1@jhmi.edu

Christopher Power
cp9@ualberta.ca

[1] Department of Mathematical and Statistical Sciences, University of Alberta, Edmonton, AB T6G 2G1, Canada

[2] Division of Neurology, Department of Medicine, University of Alberta, Edmonton, Canada

[3] Texas NeuroAIDS Research Center and Department of Pathology, University of Texas Medical Branch, Galveston, TX, USA

[4] Department of Molecular and Comparative Pathobiology and Department of Neurology, Johns Hopkins University School of Medicine, Baltimore, MD, USA

Published online: 16 May 2017

Introduction

Immunodeficiency-associated lentiviruses, human immunodeficiency virus-1 (HIV-1) and simian immunodeficiency virus (SIV), can be detected in brain tissue within weeks after primary infection (Davis et al. 1992; Witwer et al. 2009). Evidence shows HIV-1 and SIV can enter the brain through trafficking infected macrophages (Patrick et al. 2002; González-Scarano and Martin-Garcia 2005; Campbell et al. 2014). Three cell types in the brain are known to be permissive to primate lentivirus infections: astrocytes, perivascular macrophages, and microglia. Brain macrophages, including microglia and perivascular macrophages, display productive HIV-1 and SIV infections (Nowak and May 2000; Kirschner and Perelson 1995). In contrast, infected astrocytes contain viral genome but do not typically display features of active viral replication in vivo. The brain is devoid of in situ adaptive immune responses, and the blood-brain barrier (BBB) restricts antiretroviral agents from entering the brain (Annamalai et al. 2010). Thus, the brain is a natural anatomical reservoir for HIV-1 and SIV infections (Annamalai et al. 2010; Zink et al. 2010).

Both HIV-1 and SIV infections can lead to neurological disorders including HIV-associated neurocognitive disorders (HANDs), which occur in a subset of patients despite effective viral suppression in blood accompanied by restoration of $CD4^+$ T cell levels (Vivithanaporn et al. 2010). HIV-infected patients with HANDs may have lower survival rates compared with HIV-infected patients without neurological disorders (Vivithanaporn et al. 2010).

Although there is an increased appreciation and understanding of clinical aspects of HIV-1 brain infection, the underlying dynamics of viral replication and latency in the brain remain unclear. Cross-sectional autopsy studies of autopsied brain tissues revealed highly variable HIV-1 RNA levels in brain, but the impact of cART on brain viral burden remains uncertain, largely because of the relative inaccessibility of prospectively analyzed brain tissues. While mathematical modeling has been extensively used to study the dynamics of transmission and progression of HIV-1 infection of T cells in blood, few modeling studies are specific for HIV-1 or SIV brain infection (Lamers et al. 2014).

Our mathematical modeling study aimed to quantify lentiviral replication dynamics in the brain, especially among patients receiving cART. We collected and analyzed published data on HIV-1 and SIV brain infection from several studies. In a 2013 study, HIV-infected patient brain specimens from the National NeuroAIDS Tissue Consortium (NNTC) were examined for patients with advanced disease, approximately 5–15 years from primary infection (Gelman et al. 2013). Published data from three SIV studies examining macaque brain tissues without cART (Zink et al. 2010; Clements et al. 2002; Graham et al. 2011) were also included in our study. A mathematical model was formulated to describe HIV-1 and SIV infection dynamics in brain macrophages. The model was calibrated and validated using published brain data. The model showed HIV-1 and SIV infection in the brain progress slowly, due in large part to the long lifespan of infected brain macrophages. Indeed, the protracted turnover of infected brain macrophages might be an important hindrance in viral eradication (González-Scarano and Martin-Garcia 2005). Provided cART suppresses HIV-1 infection outside of the brain coupled with slow progression of HIV-1 infection in brain, moderately efficacious cART regimens could eradicate HIV-1 infection in the brain over the years.

Methods

Data

When using autopsy data for brain tissue from human cohorts, there is minimal knowledge regarding duration of infection for each patient. It is widely accepted that approximately 5–15 years from primary infection, a patient in the developed world will develop AIDS if untreated. From published studies of HIV-1 infection of the brain, we were able to ascertain data corresponding to 15 days after primary infection (Davis et al. 1992) and 5–15 years from primary infection (Gelman et al. 2013).

Brain tissue-derived data provided a large dataset from HIV/AIDS patients with advanced disease (~5–15 years from primary infection (Gelman et al. 2013)) including data from patients (n = 35) without neurological disease as determined by the NNTC neuropsychological test battery (Gelman et al. 2013); 73% of these patients were active on cART within 1 year of death. Brain-derived HIV-1 DNA data were also available from patients with HAND and/or encephalitis (n = 22); 62% were receiving cART within 1 year of death (Gelman et al. 2013).

Data used to estimate HIV-1 infected brain macrophages at primary infection for patients with and without neurological disorders came from two sources: a patient study showing positive brain HIV-1 DNA detection 15 days after primary infection (Davis et al. 1992), and the minimum of the brain-derived HIV-1 DNA data at ~5–15 years from primary infection was used as an upper bound for the estimate of the HIV-1-infected brain macrophages at primary infection (Gelman et al. 2013).

As each SIV study included brain-derived data corresponding to several time points, the three SIV studies were combined (30 macaques in total) to create a single longer time series of untreated SIV-infected brain tissue data (10, 21, 56,

and 84 days post-infection) (Zink et al. 2010; Clements et al. 2002; Graham et al. 2011). Data used for quantifying SIV-infected brain macrophages came from the brain viral DNA of this dataset. It was imperative to combine SIV studies where the macaques were the same species and each received the same strain and route of SIV infection. These three SIV studies used the same species of pigtailed macaques and were infected with the same viruses and input titers (SIV/DeltaB670/SIV/17E-Fr) (Zink et al. 2010; Clements et al. 2002; Graham et al. 2011).

Assumptions and associated data conversion

The human brain contains an estimated 171 ± 13.86 billion cells and approximately 84.6 ± 9.83 billion glial cells (Azevedo et al. 2009). A comprehensive study of the cellular composition of the gray matter of the human cerebral cortex indicated that microglia amount to only 5% of glial cells in gray matter (Herculano-Houzel 2014). From these analyses, the estimated number of microglia in the human brain is 3.74–4.72 billion cells. The average weight of a human brain is 1336 g for men and 1198 g for women (Hartmann et al. 1994). The projected number of microglia per gram of brain tissue is 2.07–3.94 million cells per gram. For the present study, the number of susceptible brain macrophages was assumed to equal the total number of microglia. Each HIV- or SIV-infected brain macrophage was assumed to contain a single copy of integrated viral DNA. Per gram of brain tissue, macaques have approximately the same number of susceptible brain macrophages as humans (Azevedo et al. 2009).

The HIV-1 and SIV studies measuring viral DNA in brain tissues used different units for measuring viral DNA. Since each HIV- or SIV-infected brain macrophage is assumed to contain a single copy of integrated viral DNA, by converting total viral DNA to integrated viral DNA (Appendix), we obtained the number of infected brain macrophages per gram of brain tissue. The conversion of HIV-1 and SIV DNA to the estimated mean number of infected brain macrophages per gram of brain tissue is displayed in Table 1 (Table 4 in the Appendix contains a full list of the converted data).

Table 1 Conversion of HIV-1 and SIV DNA to the estimated mean number of infected brain macrophages per gram of brain tissue at different times from primary infection

Virus	Neurological disorders	Estimated years infected	Mean viral DNA copies (g)	Estimated mean integrated viral DNA copies (g)	Estimated mean infected brain macrophages (g)	Ref
HIV-1	–	0.04	9–172[a]	0.1–2[a]	0.1-2[a]	Davis et al. (1992)
HIV-1	No	5–15	1.95×10^3	23	23	Gelman et al. (2013)
HIV-1	Yes	5–15	9.88×10^4	1149	1149	Gelman et al. (2013)
SIV	–	0.027	1.41×10^3	16	16	Clements et al. (2002)
SIV	–	0.058	1.24×10^3	14	14[b]	Clements et al. (2002)
SIV	–	0.058	6.22×10^3	72	72[b]	Graham et al. (2011)
SIV	17% with encephalitis	0.153	1.90×10^3	22	22	Clements et al. (2002)
SIV	83% with encephalitis	0.230	7.55×10^3	88	88	Zink et al. (2010)

[a] This study detected proviral DNA in the brain by PCR. The number of viral DNA copies was not reported. It is assumed that the level of positive detection was approximately 100 copies viral DNA per gram. The range of 9–172 copies viral DNA per gram was chosen as the data from this study

[b] The six observations from each of these studies were combined and averaged giving 43 as the mean infected brain macrophages per gram at 0.058 years infected

Mathematical model

A deterministic model using differential equations was formulated to quantify HIV-1 and SIV infection dynamics of brain macrophages. The brain macrophage population is divided into two compartments: susceptible brain macrophages, x, and infected brain macrophages, y. The infected brain macrophage population includes productively and latently infected brain macrophages. Given the limited data, it was necessary to combine productively and latently infected brain macrophages into a single compartment. HIV-1 and SIV infections of brain macrophages are assumed to spread principally through direct cell-to-cell interaction (González-Scarano and Martin-Garcia 2005; Lindl et al. 2010). Susceptible and infected brain macrophages are assumed to have homogeneous mixing. Although the brain macrophage population differs in morphology and perhaps cell density depending on the anatomic region, for the present studies, it was assumed to be uniform throughout the brain. We followed an established method of modeling direct transmission between two populations by using the rate βxy as the number of new infections per unit time, where β is the transmission coefficient (Nowak and May 2000; Kirschner and Perelson 1995). Without the presence of infection in the model, the number of susceptible brain macrophages is regulated at the equilibrium value λ/d, where λ is the source of new susceptible brain macrophages and d is the natural death rate for brain macrophages. Recent data suggest that microglia and macrophages die over months to years (Askew et al. 2017). Susceptible and infected brain macrophages were presumed to have the same death rate d because our group's earlier studies did not observe increased cellular death in HIV-infected versus uninfected brain macrophages (Walsh et al. 2014). In the HIV-1 dataset from the NNTC cohort, most patients were receiving cART within a year of death. We considered the percentage of cART effectiveness $\varepsilon \times 100\%$, where $0 \le \varepsilon \le 1$. The parameter ε is set to zero when there is no treatment.

The model is described by the set of ordinary differential equations:

$$\frac{dx}{dt} = \lambda - dx - (1-\varepsilon)\beta xy = \lambda - dx - \beta_\varepsilon xy \quad (1)$$

$$\frac{dy}{dt} = (1-\varepsilon)\beta xy - dy = \beta_\varepsilon xy - dy \quad (2)$$

where $\beta_\varepsilon = (1-\varepsilon)\beta$ is the effective transmission coefficient under cART with effectiveness ε. A more efficacious cART will result in a smaller β_ε and a lower rate of viral transmission. The variables in the model are the numbers of uninfected (x) and infected (y) brain macrophages. Model parameters λ, d, β, and ε are non-negative constants. Time units in this model are in years. Population units are the number of cells per gram of brain tissue.

This dynamic model is the mathematical translation of the current biology and biologically plausible assumptions of the lentiviral infection process in brain. It has incorporated the important causal factors and relations to quantify the infection outcomes. Effectiveness of the cART on viral transmission is incorporated in the effective transmission coefficient β_ε.

Given the initial condition of the number of infected brain macrophages at the time of infection, the model produces a temporal pattern of infected brain macrophage burden, enabling it to predict the infection outcomes. This is an important difference between a dynamic model and statistical inference models.

Compared to mathematical models for HIV-1 infection in the plasma (Nowak and May 2000; Kirschner and Perelson 1995), our model has a different transmission term. In blood leukocytes, infections occur by viral entry of host cell. In the brain, infections are assumed to occur largely by direct cell-to-cell contact (González-Scarano and Martin-Garcia 2005; Zink et al. 2010). For the same reason, unlike blood-based models for HIV-1 infection, our model does not include a compartment for free virus. Models with direct cell-to-cell transmission are also used to describe the viral dynamics of HTLV-1 infection of CD4 T cells (Nowak and May 2000; Wodarz et al. 1999; Gómez-Acevedo et al. 2010) whose lifespan is much shorter than brain macrophages. Mathematical models of HIV-1 infection of long-lived cells like macrophages were studied in Nowak and May (2000) using virus-cell interaction as the mode of transmission.

Parameter estimation and model calibration

Uniform prior distributions were specified for the parameters x_0, y_0, β_ε, and d to account for variation in estimates from the literature. The prior distribution for x_0 is estimated from the projected number of microglia per gram of brain tissue, 2.07–3.94 million cells per gram (Azevedo et al. 2009; Herculano-Houzel 2014; Hartmann et al. 1994). The minimum integrated proviral DNA burden was used as an upper bound for the prior distribution of y_0 (Zink et al. 2010; Gelman et al. 2013; Clements et al. 2002; Graham et al. 2011). The prior distribution for the transmission coefficient was given a broad range based off of general mathematical models in virology (Nowak and May 2000). The prior distribution for brain macrophage death rate d was estimated from the cellular lifespan between 1 month and 2 years (Kirschner and Perelson 1995; Askew et al. 2017). The uniform prior distributions are summarized in Table 2. The equilibrium population λ/d of susceptible brain macrophages was fitted to the per-gram amount of the brain macrophages to obtain estimation of influx λ of susceptible brain macrophages.

The parameters x_0, y_0, β_ε, and d were estimated by fitting the model predictions to the estimated per-gram numbers of infected brain macrophages at the time points in Table 4 (Appendix). Three datasets in Table 4, excluding outliers,

Table 2 Uniform prior distributions for parameters estimated from literature for both humans and macaques

Datasets	Symbol	Parameter	Prior distribution	Unit	Ref
HIV-1 without neurological disorders	x_0	Initial value for x	U(2.07×10^6, 3.94×10^6)	per g	Azevedo et al. (2009); Herculano-Houzel (2014); Hartmann et al. (1994)
	y_0	Initial value for y	U(0, 2)	per g	Gelman et al. (2013)
	$\beta_{\bar{\varepsilon}}$	Transmission coefficient	U(1×10^{-8}, 1×10^{-5})	per year	Nowak and May (2000)
	d	Death rate brain macrophages	U(0.5, 10.22)	per year	Kirschner and Perelson (1995)
HIV-1 with neurological disorders	x_0	Initial value for x	U(2.07×10^6, 3.94×10^6)	per g	Azevedo et al. (2009); Herculano-Houzel (2014); Hartmann et al. (1994)
	y_0	Initial value for y	U(0, 9.5)	per g	Gelman et al. (2013)
	$\beta_{\bar{\varepsilon}}$	Transmission coefficient	U(1×10^{-8}, 1×10^{-5})	per year	Nowak and May (2000)
	d	Death rate brain macrophages	U(0.5, 10.22)	per year	Kirschner and Perelson (1995)
SIV	x_0	Initial value for x	U(2.07×10^6, 3.94×10^6)	per g	Azevedo et al. (2009); Herculano-Houzel (2014); Hartmann et al. (1994)
	y_0	Initial value for y	U(0, 2)	per g	Zink et al. (2010); Clements et al. (2002); Graham et al. (2011)
	β_0	Transmission coefficient	U(1×10^{-8}, 1×10^{-4})	per year	Nowak and May (2000)
	d	Death rate brain macrophages	U(0.5, 10.22)	per year	Kirschner and Perelson (1995)

were used to produce three sets of estimated parameter values in Table 3, for three study cohorts: cART-treated HIV-1-infected patients without neurological disorders, cART-treated HIV-1-infected patients with neurological disorders, and untreated SIV infected macaques. Since there is minimal knowledge regarding duration of infection for each patient, the model was fit to the cART-treated HIV-1 patient data at 5, 10, and 15 years from primary infection (estimated

Table 3 Fitted parameter estimates and 95% credible intervals for the model fit to three datasets

Datasets	Symbol	Parameter	Estimate (95% credible interval)	Unit
HIV-1 without neurological disorders (fit at 5, 10, 15 years)	x_0	Initial value for x	2.33×10^6 2.07×10^6–3.94×10^6	per gm
	y_0	Initial value for y	0.136 0.0246–2.00	per gm
	$\beta_{\bar{\varepsilon}}$	Transmission coefficient	2.23×10^{-6} 2.90×10^{-7}-4.87×10^{-6}	per year
	d	Death rate brain macrophages	4.72 0.542–10.2	per year
HIV-1 with neurological disorders (fit at 5, 10, 15 years)	x_0	Initial value for x	2.39×10^6 2.07×10^6–3.94×10^6	per gm
	y_0	Initial value for y	9.05 0.0416–9.50	per gm
	$\beta_{\bar{\varepsilon}}$	Transmission coefficient	3.17×10^{-6} 2.76×10^{-7}-5.60×10^{-6}	per year
	d	Death rate brain macrophages	6.88 0.501–10.2	per year
SIV	x_0	Initial value for x	2.28×10^6 2.09×10^6–3.94×10^6	per gm
	y_0	Initial value for y	1.99 1.76–2.00	per gm
	β_0	Transmission coefficient	1.03×10^{-5} 5.30×10^{-6}-1.37×10^{-5}	per year
	d	Death rate brain macrophages	3.30 0.743–9.98	per year

parameter values including the outliers are presented in Table 5 in the Appendix).

The method of Bayesian inference was implemented for the model fitting and is described in the Appendix. Posterior distributions from Bayesian inference were used to produce the mean value and 95% credible intervals of the fitted parameters.

Sensitivity and uncertainty analysis

The 95% credible intervals of the fitted parameters obtained from Bayesian inference, using Markov Chain Monte Carlo (MCMC) sampling, were used to measure sensitivity of model outcomes with respect to variations in these four parameters. To demonstrate uncertainty in our predictions with respect to variations of parameter values, the Latin Haypercube Sampling (LHS) method was used to sample values of sensitive parameters within their credible intervals, and sampled parameter values were used to produce the dark gray bands in Figs. 1, 2, and 3. The 95% prediction intervals from the MCMC sampling are shown in Fig. 1 with the dashed light gray curves.

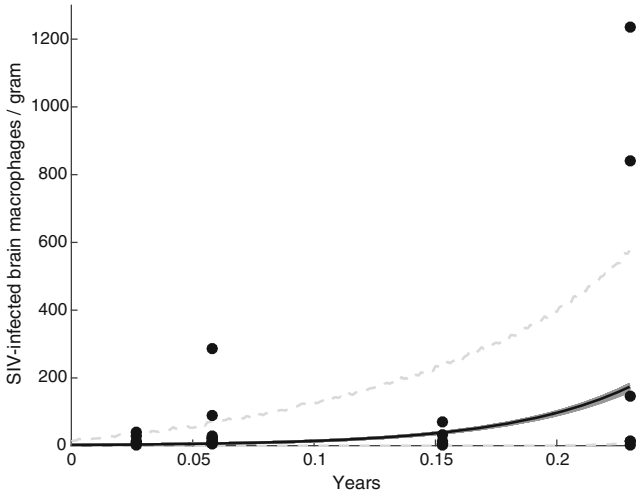

Fig. 2 Infected brain macrophage burden for SIV-infected (untreated) macaques. The *black points* are the observed data, the *black curve* is the mean model solution, the *dark gray region* is the 95% credible interval for the model solutions, and the *dashed light gray curves* indicate the 95% prediction interval

Results

The fitted parameter estimates for x_0, y_0, β_ε and d, together with their 95% credible intervals, are shown in Table 3. For the cART-treated HIV-1 patient data, the 95% credible intervals for the fitted parameter estimates include the variation from the model fit to 5, 10, and 15 years from primary infection (the best fit parameter estimates correspond to 10 years from primary infection).

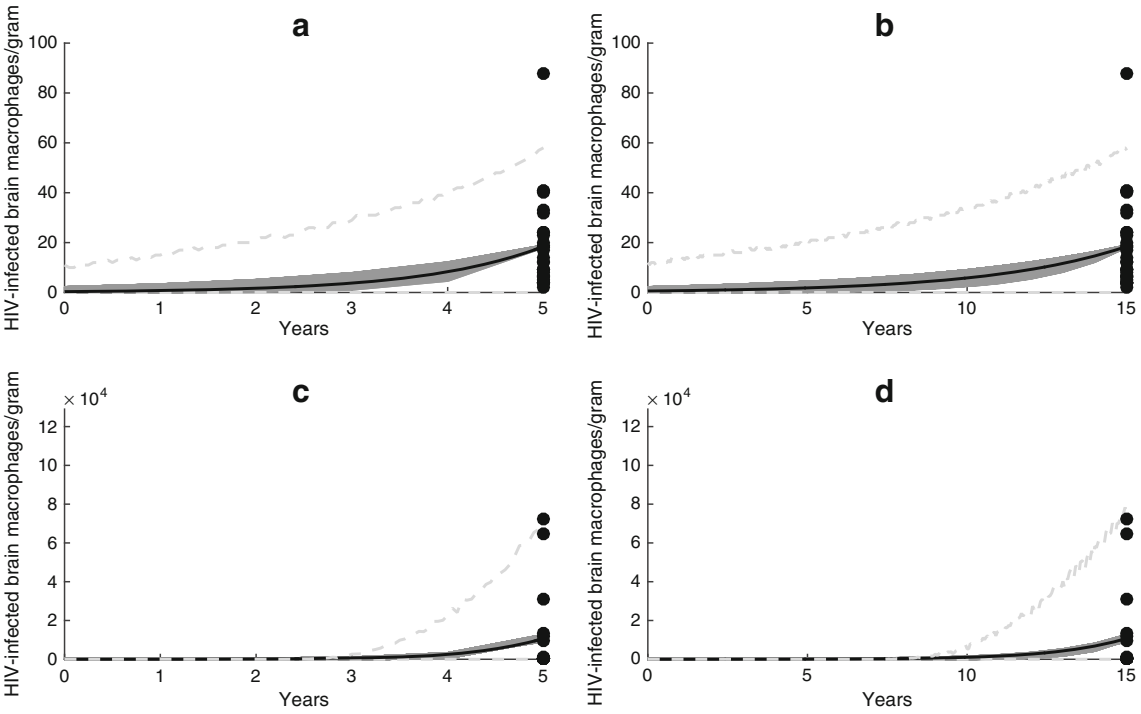

Fig. 1 Infected brain macrophage burden. cART-treated HIV-infected patients without neurological disorders fit at **a** 5 years and **b** 15 years from primary infection. cART-treated HIV-infected patients with neurological disorders fit at **c** 5 years and **d** 15 years from primary infection. The *black points* are the observed data, the *black curve* is the mean model solution, the *dark gray region* is the 95% credible interval for the model solutions, and the *dashed light gray curves* indicate the 95% prediction interval

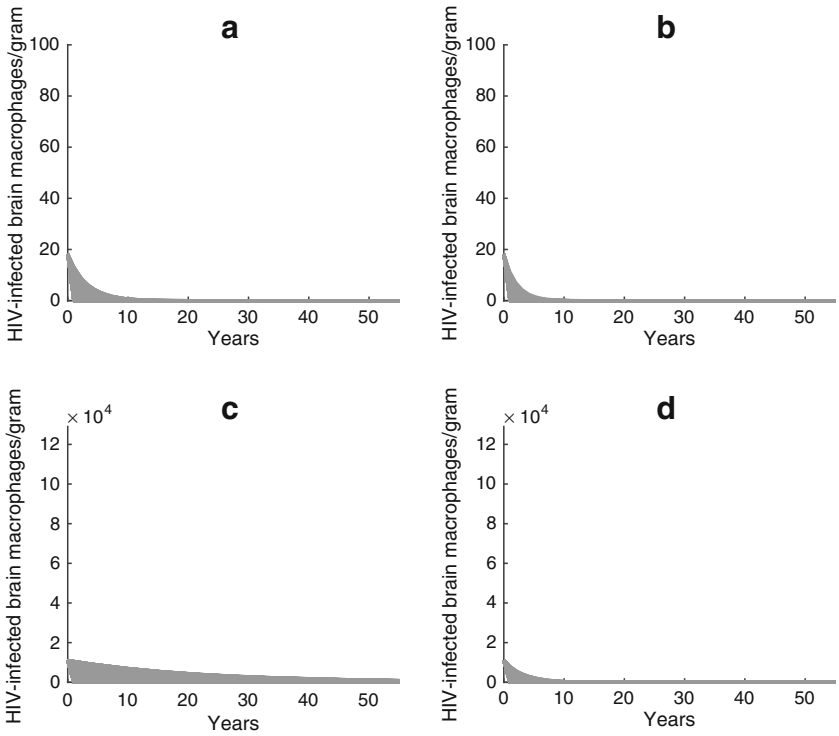

Fig. 3 HIV-1 infected brain macrophage burden with cART. Assuming a 70% improved efficiency in cART from the baseline. Late-presenting patients without neurological disorders fit at **a** 5 years and 15 years (**b**), and late-presenting patients with neurological disorders fit at **c** 5 years and 15 years (**d**) will show differing durations to the time of eradication. Curves lying in the *dark gray region* represent the 95% credible interval for the model solutions

HIV-1 infection of brain macrophages progresses slowly

The HIV-1 infected brain macrophage burden for patients without neurological disorders is displayed in Fig. 1a for 5 years and Fig. 1b for 15 years post-infection. The HIV-1 infected brain macrophage burden for patients with neurological disorders is displayed in Fig. 1c for 5 years and Fig. 1d for 15 years post-infection. SIV-infected brain macrophage burden for untreated macaques is shown in Fig. 2.

The estimated values of the transmission coefficient β_ε in Table 3 were used to compare the viral transmission rates in brain for cART-treated HIV-infected patients with and without neurological disorders. The 95% credible interval for HIV-1 transmission rate overlaps for cART-treated HIV-infected patients with and without neurological disorders. The upper bound of the HIV-1 transmission rate was 19.3 times higher for cART-treated HIV-infected patients with neurological disorders compared to those without neurological disorders. When compared to the transmission coefficient for HIV-1 infection in the plasma in the literature (Althaus et al. 2014), we found that the HIV-1 transmission rate among $CD4^+$ T cells was 2.0–3.3$\log_{10}$ fold higher than HIV-1 infection among brain macrophages. These findings suggest the progression of HIV-1 infection in the brain was slower in comparison to HIV-1 infection in the plasma (Althaus et al. 2014). The transmission rate for SIV infection among untreated macaques was estimated to be 5.30×10^{-6}–1.37×10^{-5} per year.

Combination antiretroviral therapy

The control reproduction number, R_ε:

$$R_\varepsilon = (1-\varepsilon)\frac{\beta\lambda}{d^2} = \frac{\beta_\varepsilon\lambda}{d^2} \tag{3}$$

where $\beta_\varepsilon = (1-\varepsilon)\beta$. The parameter ε represents cART effectiveness. The parameter ε is set to zero when there is no treatment. In a fully susceptible brain macrophage population, the average number of newly infected brain macrophages caused by a single infected brain macrophage during its infectious lifetime is given by the basic reproduction number, R_0.

The R_0 estimated value for untreated SIV-infected macaques was determined to be 2.91–27.0. In the literature, the R_0 value for untreated SIV-infected macaques in the plasma has a range of 2–68 (Nowak et al. 1997). For the infection to decline in the brain for untreated SIV-infected macaques, it is necessary to have $\varepsilon > 0$. To inhibit replication in the brain for untreated SIV-infected macaques, the minimum cART effectiveness was estimated to be 65.61–96.30% ($0.6561 \le \varepsilon \le 0.9630$).

The baseline effectiveness $\overline{\varepsilon}$ of the current cART for HIV-1 infection in brain is not known, neither was the basic reproduction number R_0 for the untreated patients. We used the estimated value of the effective transmission coefficient $R_{\overline{\varepsilon}}$ as a substitute for baseline effectiveness and used $R_\varepsilon/R_{\overline{\varepsilon}}$ for comparison of efficacies ε and $\overline{\varepsilon}$.

The estimated 95% credible interval for $R_{\bar{\varepsilon}}$ was 1.02–1.91 with interquartile range of 1.03–1.21 for cART-treated patients without neurological disorders. The estimated 95% credible interval for $R_{\bar{\varepsilon}}$ was 1.05–3.15 with interquartile range of 1.07–1.56 for cART-treated patients with neurological disorders. In comparison, the R_0 value for untreated HIV-1 infection in the plasma has median 8.0 and interquartile range 4.9–11 (Ribeiro et al. 2010). In the literature, a cART effectiveness of 0.85 would suppress the viral load in the plasma to undetectable levels after a few months (Rong and Perelson 2009). Using a cART effectiveness of 0.85 and the R_0 value for untreated HIV-1 infection in the plasma with range 4.9–11 (Ribeiro et al. 2010), the value of $R_{0.85}$ for treated HIV-1 infection in the plasma would be in the interquartile range of 0.74–1.65. The estimated interquartile range of $R_{\bar{\varepsilon}}$ in the brain for cART-treated patients was 1.03–1.56 and lies in the interquartile range of $R_{0.85}$ for infection in the plasma.

For the infection to decline in the brain of cART-treated patients, it is necessary to have $\varepsilon > \bar{\varepsilon}$. To inhibit replication in the brain ($R_{\varepsilon} < 1$), the minimum improvement in cART effectiveness from the baseline was estimated to be 1.652–47.70% for patients without neurological disorders, and 4.807–68.24% for patients with neurological disorders.

Provided cART suppresses HIV-1 infection outside the brain, and with a 70% improvement in cART efficiency in the brain, it would require 3–32 years (interquartile range 3–9) to reduce the number of infected brain macrophages to approximately 0.001 cells per gram for a late diagnosed patient without neurological disorders (Fig. 3a for model fit to 5 years and Fig. 3b 15 years post-infection), and it would require 4–51 years (interquartile range 4–16) for the same reduction for a late diagnosed patient with neurological disorders (Fig. 3c for model fit to 5 years and Fig. 3d 15 years post-infection).

Discussion

To our knowledge, this is the first mathematical modeling study to quantify HIV-1 and SIV infection dynamics in the brain. Our modeling study indicates that HIV-1 and SIV provirus burdens in brain increase slowly over time. Assuming antiretroviral therapy suppresses HIV-1 infection outside the brain, an efficacious antiretroviral therapy could eradicate HIV-1 infection in the brain, albeit over a decade for patients without neurological complications and over two decades for those with HAND.

We focused on brain viral DNA as a marker of infected cells in contrast to brain viral RNA. Brain viral RNA levels varied widely over time (Zink et al. 2010; Gelman et al. 2013; Clements et al. 2002; Graham et al. 2011). Brain viral DNA levels displayed less variability and were determined to be a stable indicator of infection. We relied on data from a study examining human brain specimens from the NNTC; these data provided findings from patients with advanced disease (Gelman et al. 2013). This latter study reported that brain viral RNA was higher in patients with neurological disorders, HAND and HIVE, than in patients without neurological disorders and that brain viral RNA and DNA levels were correlated with worse neuropsychological performance (Gelman et al. 2013). We used two sources to gain insight into the state of brain infection during primary infection: we used the study of a single HIV-infected patient, who was infected 15 days after iatrogenic HIV-1 infection and HIV-1 was detected in the brain (Davis et al. 1992), and the minimum of the brain-derived HIV-1 DNA data at ~5–15 years from primary infection was used as an upper bound for the estimate of the HIV-1 infected brain macrophages at primary infection (Gelman et al. 2013). Additionally, our predictions of SIV brain viral burden at the time of initial/primary infection are congruent with the number used herein for humans. A study not included in our research was a paper examining the brain viral DNA and brain viral RNA of 15 patients (Johnson et al. 1996). In this study, there was no significant difference in brain viral DNA between patients with and without neurological disorders (Johnson et al. 1996). This result is later contradicted by a study examining a larger sample size of 195 patients (Gelman et al. 2013).

In blood-derived lymphocytes, the average ratio of integrated proviral DNA to total viral DNA is 1:86 (Suspène and Meyerhans 2012). We used this ratio as an estimate for the average ratio of integrated proviral DNA to total viral DNA in brain macrophages. An earlier study found the ratio of integrated proviral DNA to total viral DNA in brain tissues from HIV-1 encephalitis cases ranged from 1:6 to 1:81 (Pang et al. 1990). The average ratio in blood and the ratio in brain tissues from HIV-1 encephalitis patients are the same order of magnitude. In the present study, changing this ratio of integrated proviral DNA to total viral DNA would affect the estimated mean integrated viral DNA copies per gram of brain tissue used to fit the mathematical model. In the extreme case of 1:6 being the ratio of integrated proviral DNA to total viral DNA, there was an estimated 8–12% difference between the new transmission coefficient and the transmission coefficient estimated under the ratio assumption of 1:86.

Brain tissue measurements from an HIV-1 infected patient are very rarely available before death. Two major limitations in using autopsy data for brain tissue from human cohorts are minimal knowledge regarding durations of infection and antiretroviral therapy for each patient. An estimate for the duration of infection for each patient in the autopsy data assumes each patient has AIDS and died at least 10 years after primary infection whether or not a patient is active on antiretroviral therapy within 1 year of death. An issue not addressed herein is viral burden in cerebrospinal fluid (CSF); many studies

have reported on HIV-1 RNA levels in CSF, albeit usually free virus particles (Nightingale et al. 2014). CSF as an indicator of viral dynamics within brain has substantial challenges because the relative paucity of cells in CSF compounded by the predominance of lymphocytes in CSF, presumably derived from blood, making it a questionable surrogate indicator of brain virus-related events. However, it would be valuable to have a better understanding of brain-CSF correlations in viral replication and latency in the future management of patients receiving cART.

The obstacles in obtaining accurate estimates for the durations of infection and antiretroviral therapy for individual patients necessitates the use of SIV studies where the durations of infection and antiretroviral therapy are known for each macaque. Our SIV data comes from the same animal model (Zink et al. 2010; Clements et al. 2002; Graham et al. 2011). Thus, the present SIV results may be specific to this animal model. We used published experimental data from three SIV studies that examined macaque brains at different times post-infection (p.i.) (Zink et al. 2010; Clements et al. 2002; Graham et al. 2011). One SIV study found that brain viral DNA levels remained at constant levels from the acute phase through the asymptomatic period (Clements et al. 2002). A further SIV study demonstrated that cART was capable of reducing brain viral RNA to undetectable levels but had little impact on brain viral DNA levels after acute infection (Zink et al. 2010). The last included SIV study reported that cART greatly reduced viral RNA levels but exerted little effect on viral DNA levels at 21 days p.i. (Graham et al. 2011). The current mathematical investigations indicated that the mathematical model adequately fits the experimental in vivo SIV data. This modeling strategy could be applied to SIV datasets from other animal models, yielding insights into the viral progression rate in brain macrophages from primary infection.

A 0.85 cART effectiveness would suppress the viral load in the plasma to undetectable levels after a few months (Rong and Perelson 2009). If cART effectiveness was 0.85 within the brain ($\bar{\varepsilon} = 0.85$), the R_0 value in the brain for untreated patients would be in the interquartile range 6.87–10.4, similar to the R_0 interquartile range for untreated HIV-1 infection in the plasma 4.9–11. Yet, the blood-brain barrier restricts some antiretroviral agents from entering the brain (Annamalai et al. 2010) and a 0.85 cART effectiveness in the brain would most likely be too high an effectiveness. If cART effectiveness was less than 0.85 ($\bar{\varepsilon} < 0.85$), the small value of $R_{\bar{\varepsilon}}$ in the brain for cART-treated patients 1.03–1.56 might be due to a slower progression of HIV-1 infection in the brain in comparison to HIV-1 infection in the plasma.

Because of the limited data available for HIV-1 and SIV brain infection, it was necessary to use a simple mathematical model that restricted the number of model parameters needed to fit the empiric data. Although microglia and trafficking macrophages might behave differently, these cell populations were treated as the single cell population of brain macrophages. Although astrocytes constitute a large proportion of cells in the human brain, astrocytes were not considered in this study because astrocytes have a limited infection and produce little or no virus (Gray et al. 2014). Also, previous data suggest that antiretroviral therapy effectively suppresses viral production in astrocytes (Gray et al. 2013). Notwithstanding the restricted infection of astrocytes, their infection does lead to cellular dysfunction and contributes to neurological disorders (Gray et al. 2014). Our model considers microglia and trafficking macrophages capable of full replication. A model incorporating astrocytes would be beneficial in future modeling studies. Different anatomical areas within the brain contain variable levels of HIV-1- and SIV-infected cells during disease progression (Kure et al. 1990). In this model, it is assumed that the infected brain macrophage population is distributed homogeneously across the entire brain; moreover, an infected brain macrophage might be productively or latently infected. The model does not make this distinction for infected brain macrophages. Viral rebound, non-compliance to cART, brain penetration of cART, and type of cART used are important considerations; given the available data, these issues were not included in the model. We elected not to study CSF viral load or cell-free virus in this analysis because we focused on brain viral tissue dynamics during infection in this study. Despite these simplifications, our model provides an estimate of the HIV-infected brain macrophage burden from primary infection and the necessary improvements in current cART regimens needed to curtail and eventually eliminate HIV-1 infection from the brain.

Future studies are warranted to model both productively and latently infected brain macrophages using the viral DNA and viral RNA data. This approach would allow a more accurate estimation of cART effectiveness. The application of HIV-infected humanized mice with and without cART might facilitate this effort (Araínga et al. 2016). Creating a model to quantify viral infection in specific areas of the brain over time would also be informative, as it would permit determination of which regions of the brain display the largest viral burden over the course of infection and how cART might be optimized to ensure rapid eradication of virus from the brain.

Acknowledgements The authors thank Mr. William Branton for the technical information, Ms. Suzanne E. Queen for the database assistance, and Dr. Arianna Bianchi for the useful suggestion about predictive interval. This work was supported by the NSERC, CIHR, CFI, and Alberta Innovates-Health Solutions. BG acknowledges support from NIH grants U24MH100930 and R01MH101017.

Compliance with ethical standards

Support for the work ELA holds fellowship awards from the Canadian Institutes of Health Research and Alberta Innovates-Health Solutions. CP holds a Canada Research Chair in Neurological Infection and Immunity. Research for MYL is supported in part by grants from the Natural Science and Engineering Research Council of Canada (NSERC) and Canada Foundation for Innovation (CFI).

Conflict of interest The authors declare that they have no conflict of interest.

References

Althaus CL, Joos B, Perelson AS, Günthard HF (2014) Quantifying the turnover of transcriptional subclasses of HIV-1-infected cells. PLoS Comput Biol 10(10):e1003871

Annamalai L, Bhaskar V, Pauley DR, Knight H, Williams K, Lentz M et al (2010) Impact of short-term combined antiretroviral therapy on brain virus burden in simian immunodeficiency virus-infected and $CD8^+$ lymphocyte-depleted rhesus macaques. Am J Pathol 177(2): 777–791

Araínga M, Hang S, Poluektova LY, Gorantla S, Gendelman HE (2016) HIV-1 cellular and tissue replication patterns in infected humanized mice. Sci Rep 6:23513

Askew K, Li K, Olmos-Alonso A, Garcia-Moreno F, Liang Y, Richardson P et al (2017) Coupled proliferation and apoptosis maintain the rapid turnover of microglia in the adult brain. Cell Rep 18(2):391–405

Azevedo FAC, Carvalho LRB, Grinberg LT, Farfel JM, Ferretti REL, Leite REP et al (2009) Equal numbers of neuronal and nonneuronal cells make the human brain an isometrically scaled-up primate brain. J Comp Neurol 513:532–541

Campbell JH, Ratai EM, Autissier P, Nolan DJ, Tse S, Miller AD et al (2014) Anti-α4 antibody treatment blocks virus traffic to the brain and gut early, and stabilizes CNS injury late in infection. PLoS Pathog 10(12):1–15

Clements JE, Babas T, Mankowski JL, Suryanarayana K, Piatak M Jr, Tarwater PM et al (2002) The central nervous system as a reservoir for simian immunodeficiency virus (SIV): steady-state levels of SIV DNA in brain from acute through asymptomatic infection. J Infect Dis 186:905–913

Davis LE, Hjelle BL, Miller VE, Palmer DL, Llewellyn AL, Merlin TL et al (1992) Early viral brain invasion in iatrogenic human immunodeficiency virus infection. Neurology 42:1736–1739

Gelman BB, Lisinicchia JG, Morgello S, Masliah E, Commins D, Achim CL et al (2013) Neurovirological correlation with HIV-associated neurocognitive disorders and encephalitis in a HAART-era cohort. J Acquir Immune Defic Syndr 62(5):487–495

Gómez-Acevedo H, Li MY, Jacobson S (2010) Multistability in a model for CTL response to HTLV-I infection and its implications to HAM/TSP development and prevention. Bull Math Biol 72(3):681–696

González-Scarano F, Martin-Garcia J (2005) The neuropathogenesis of AIDS. Nat Rev Immunol 5:69–81

Graham DR, Gama L, Queen SE, Li M, Brice AK, Kelly KM et al (2011) Initiation of HAART during acute simian immunodeficiency virus infection rapidly controls virus replication in the CNS by enhancing immune activity and preserving protective immune responses. J Neuro-Oncol 17:120–130

Gray LR, Tachedjian G, Ellett AM, Roche MJ, Cheng WJ, Guillemin GJ et al (2013) The NRTIs lamivudine, stavudine, zidovudine have reduced HIV-1 inhibitory activity in astrocytes. PLoS One 8(4): e62196

Gray LR, Turville SG, Hltchen TL, Cheng WJ, Ellett AM, Salimi H et al (2014) HIV-1 entry and trans-infection of astrocytes involves CD81 vesicles. PLoS One 9(2):e90620

Hartmann P, Ramseier A, Gudat F, Mihatsch MJ, Polasek W (1994) Normal weight of the brain in adults in relation to age, sex, body height and weight [abstract]. Pathologe 15(3):165–170

Herculano-Houzel S (2014) The glia/neuron ratio: how it varies uniformly across brain structures and species and what that means for brain physiology and evolution. Glia 62:1377–1391

Johnson RT, Glass JD, McArthur JC, Chesebro BW (1996) Quantitation of human immunodeficiency virus in brains of demented and nondemented patients with acquired immunodeficiency syndrome. Ann Neurol 39(3):392–395

Kirschner DE, Perelson AS (1995) A model for the immune system response to HIV: AZT treatment studies. In: Arino O, Axelrod DE, Kimmel M, Langlais M (eds) Mathematical population dynamics: analysis of heterogeneity, vol. 1, theory of epidemics. Wuerz Publishing Ltd, Winnipeg, pp 295–310

Kure K, Weidenheim KM, Lyman WD, Dickson DW (1990) Morphology and distribution of HIV-1 gp41-positive microglia in subacute AIDS encephalitis. Pattern of involvement resembling a multisystem degeneration. Acta Neuropathol 80:393–400

Lamers SL, Fogel GB, Nolan DJ, McGrath MS, Marco S (2014) HIV-associated neuropathogenesis: a systems biology perspective for modeling and therapy. Biosystems 119:53–61

Lindl KA, Marks DR, Kolson DL (2010) HIV-associated neurocognitive disorder: pathogenesis and therapeutic opportunities. J NeuroImmune Pharmacol 5:294–309

Nightingale S, Winston A, Letendre S, Michael BD, McArthur JC, Khoo S et al (2014) Controversies in HIV-associated neurocognitive disorders. Lancet Neurol 13(11):1139–1151

Nowak MA, May RM (2000) Virus dynamics. Mathematical principles of immunology and virology. Oxford University Press, Oxford

Nowak MA, Lloyd AL, Vasquez GM, Wiltrout TA, Wahl LM, Bischofberger N et al (1997) Viral dynamics of primary viremia and antiretroviral therapy in simian immunodeficiency virus infection. J Virol 71(10):7518–7525

Pang S, Koyanagi Y, Miles S, Wiley C, Vinters HV, Chen ISY (1990) High levels of unintegrated HIV-1 DNA in brain tissue of AIDS dementia patients. Nature 343(6253):85–89

Patrick MK, Johnston JB, Power C (2002) Lentiviral neuropathogenesis: comparative neuroinvasion, neurotropism, neurovirulence, and host neurosusceptibility. J Virol 76(16):7923–7931

Ribeiro RM, Qin L, Chavez LL, Li D, Self SG, Perelson AS (2010) Estimation of the initial viral growth rate and basic reproductive number during acute HIV-1 infection. J Virol 84(12):6096–6102

Rong L, Perelson AS (2009) Modeling latently infected cell activation: viral and latent reservoir persistence, and viral blips in HIV-infected patients on potent therapy. PLoS Comput Biol 5(10):e1000533

Suspène R, Meyerhans A (2012) Quantification of unintegrated HIV-1 DNA at the single cell level *in vivo*. PLoS One 7(5):e36246

Vivithanaporn P, Heo G, Gamble J, Krentz HB, Hoke A, Gill MJ et al (2010) Neurologic disease burden in treated HIV/AIDS predicts survival. Neurology 75:1150–1158

Walsh JG, Reinke SN, Mamik MK, McKenzie BA, Maingat F, Branton WG et al (2014) Rapid inflammasome activation in microglia contributes to brain disease in HIV/AIDS. Retrovirology 11:35

Witwer KW, Gama L, Li M, Bartizal CM, Queen SE, Varrone JJ et al (2009) Coordinated regulation of SIV replication and immune responses in the CNS. PLoS One 4(12):e8129

Wodarz D, Nowak MA, Bangham CR (1999) The dynamics of HTLV-I and the CTL response. Immunol Today 20(5):220–227

Zink MC, Brice AK, Kelly KM, Queen SE, Gama L, Li M et al (2010) Simian immunodeficiency virus-infected macaques treated with highly active antiretroviral therapy have reduced central nervous system viral replication and inflammation but persistence of viral DNA. J Infect Dis 202(1):161–170